Quantifying the Dynamics of HIV Decline in Perinatally Infected Neonates on Antiretroviral Therapy

Sinead E. Morris, PhD,[a] Luise Dziobek-Garrett, MSc,[a,b] Renate Strehlau, MBBCh,[c] Juliane Schröter, MSc,[d] Stephanie Shiau, PhD, MPH,[e,f] Anet J. N. Anelone, PhD,[d,g] Maria Paximadis, PhD,[h] Rob J. de Boer, PhD,[d] Elaine J. Abrams, MD,[f,i,j] Caroline T. Tiemessen, PhD,[h] Louise Kuhn, PhD, MPH,[e,f] and Andrew J. Yates, PhD,[a] on behalf of the EPIICAL Consortium and the LEOPARD study team

Background: Mathematical modeling has provided important insights into HIV infection dynamics in adults undergoing antiretroviral treatment (ART). However, much less is known about the corresponding dynamics in perinatally infected neonates initiating early ART.

Setting: From 2014 to 2017, HIV viral load (VL) was monitored in 122 perinatally infected infants identified at birth and initiating ART within a median of 2 days. Pretreatment infant and maternal covariates, including CD4 T cell counts and percentages, were also measured.

Methods: From the initial cohort, 53 infants demonstrated consistent decline and suppressed VL below the detection threshold (20 copies mL^{-1}) within 1 year. For 43 of these infants with sufficient VL data, we fit a mathematical model describing the loss of short-lived and long-lived infected cells during ART. We then estimated the lifespans of infected cells and the time to viral suppression, and tested for correlations with pretreatment covariates.

Results: Most parameters governing the kinetics of VL decline were consistent with those obtained previously from adults and other infants. However, our estimates of the lifespan of short-lived infected cells were longer than published values. This difference may reflect sparse sampling during the early stages of VL decline, when the loss of short-lived cells is most apparent. In addition, infants with higher pretreatment CD4 percentage or lower pretreatment VL trended toward more rapid viral suppression.

Conclusions: HIV dynamics in perinatally infected neonates initiating early ART are broadly similar to those observed in other age groups. Accelerated viral suppression is also associated with higher CD4 percentage and lower VL.

Key Words: HIV, neonates, ART, mathematical model, viral dynamics, biphasic decay

(*J Acquir Immune Defic Syndr* 2020;85:209–218)

Received for publication January 19, 2020; accepted May 18, 2020.

From the [a]Department of Pathology and Cell Biology, Columbia University Medical Center, New York, NY; [b]Office of University Investments, Cornell University, New York, NY 10032 ; [c]Department of Paediatrics and Child Health, Empilweni Services and Research Unit, Rahima Moosa Mother and Child Hospital, Faculty of Health Sciences, University of the Witwatersrand, Johannesburg, South Africa; [d]Department of Theoretical Biology and Bioinformatics, Utrecht University, Utrecht, Netherlands; [e]Gertrude H. Sergievsky Center, Vagelos College of Physicians and Surgeons, Columbia University Medical Center, New York, NY; [f]Department of Epidemiology, Mailman School of Public Health, Columbia University Medical Center, New York, NY; [g]School of Mathematics and Statistics, University of Sydney, Sydney, Australia; [h]Centre for HIV and STIs, National Institute for Communicable Diseases, National Health Laboratory Services, and Faculty of Health Sciences, University of the Witwatersrand, Johannesburg, South Africa; [i]ICAP at Columbia University, Mailman School of Public Health, Columbia University Medical Center, New York, NY; and [j]Department of Pediatrics, Vagelos College of Physicians & Surgeons, Columbia University Medical Center, New York, NY.

This work is part of the EPIICAL project (http://www.epiical.org/), supported by the PENTA-ID foundation (http://penta-id.org/), funded through an independent grant by ViiV Healthcare UK.

Presented in part at: Second EPIICAL General Assembly; November 14–16, 2018; Madrid, Spain; Ecology and Evolution of Infectious Diseases conference, Princeton University; June 10–13, 2019; Princeton, NJ; fourth Workshop on Viral Dynamics; October 21–23, 2019; Paris, France.

The authors have no conflicts of interest to disclose.

Conceptualization: S.E.M., L.D.-G., R.J.d.B., J.S., A.J.N.A., and A.J.Y. Data analysis: S.E.M. and L.D.-G. Study design and conduct of the original study: R.S., S.S., M.P., C.T.T., E.J.A., and L.K. Writing of the article: S.E.M. and A.J.Y. Critical input into interpretation of results: all authors. Editing and approval of the article: all authors.

Supplemental digital content is available for this article. Direct URL citations appear in the printed text and are provided in the HTML and PDF versions of this article on the journal's Web site (www.jaids.com).

EPIICAL Consortium and the LEOPARD study team members are listed in ACKNOWLEDGMENTS section.

Correspondence to: Sinead E. Morris, Department of Pathology and Cell Biology, Columbia University Medical Center, New York, NY 10032 (e-mail: sinead.morris@columbia.edu).

INTRODUCTION

In 2017, was responsible for the deaths of 1 million people globally, including 50,000 children less than 1 year old.[1,2] Although numerous studies have shown that antiretroviral treatment (ART) can improve prognosis when initiated early in infancy,[3–12] the extent to which this applies during the neonatal period is less clear.[13] Determining optimal ART approaches and the clinical factors associated with successful outcomes are particularly important for perinatally infected neonates who face high levels of mortality in the absence of treatment.[14]

In adults, mathematical modeling has provided many insights into the dynamics of HIV infection during treatment.

For example, simple frameworks describing the time course of viral load (VL) have identified distinct populations of infected cells (such as CD4 T cells) that decay at different rates and differentially impact overall viremia.[15–20] These models accurately capture the classic "biphasic" kinetics of viral decline, with an initial fast phase dominated by the rapid loss of short-lived infected cells and a second slower phase driven by the loss of other, longer-lived infected cells.[15,16,21] Notably, modeling has shown that over 90% of all infected cells in chronically infected adults are short-lived, with an average lifespan of 1 day, revealing the highly dynamic nature of HIV infection.[16]

Despite the extensive characterization of infected cell populations in adults on ART, much less is known about the corresponding dynamics in younger age groups. This is partly due to limitations in the frequency and size of blood draws used to measure VL and/or target cell populations. Nevertheless, one study of infants aged 15 days to 2 years found a consistent biphasic pattern of viral decay during ART, similar to that described in adults.[22] In addition, infants less than 3 months of age had slower rates of viral decay than those older than 3 months, suggesting important differences in viral dynamics, ART efficacy, or immune responses very early in life. However, it is unclear whether these findings extend to other cohorts, particularly perinatally infected infants undergoing ART in the first weeks of life.

In this study, we model the dynamics of HIV infection in a cohort of perinatally infected infants in Johannesburg, South Africa, most of whom initiated ART as neonates.[23] We estimate the lifespans of key infected cell populations and the time at which infants achieve viral suppression. In general, we find the lifespans of short-lived infected cells are longer than those found in adults and other infants, whereas all other parameters are similar. The former result may reflect poor drug efficacy and/or immune responses in neonates or, alternatively, insufficient sampling during the highly dynamic phase of initial viral decline. In addition, we find that infants with higher pretreatment CD4 percentage or lower pretreatment VL trend toward achieving faster suppression. Overall, our results suggest that HIV dynamics in perinatally infected neonates on ART are not substantially different to those observed in other age groups.

METHODS

Data

From 2014 to 2017, 122 perinatally infected infants were enrolled in the study at the Rahima Moosa Mother and Child Hospital in Johannesburg, South Africa. Most began ART within 2 weeks of birth [median age = 2.5 days; interquartile range (IQR) = 1–8 days] and were followed up to 4 years to measure VL in response to treatment.[23] A number of pretreatment (referred to as "baseline") covariates were concurrently recorded, including sex, birth weight, CD4 count and percentage, and the VL of both the infant and mother (full list in the Supplemental Digital Content, http://links.lww.com/QAI/B497).

To analyze the dynamics of viral decline, we only considered infants who reached suppression within the first year of life, defined here as having at least 1 VL measurement below the 20 copies mL^{-1} detection threshold of the RNA assay. All measurements below this threshold were set to 10 copies mL^{-1} in line with previous work[24], and using alternative values did not substantially impact our results (see Supplemental Digital Content, http://links.lww.com/QAI/B497). To isolate the kinetics leading to initial suppression, VL time courses were truncated after the first measurement below the detection threshold. We also investigated alternative criteria that defined suppression as sustaining at least 2 consecutive VL measurements below the detection threshold. This more restrictive definition gave similar qualitative conclusions to the less stringent criteria (see Supplemental Digital Content, http://links.lww.com/QAI/B497), and so, we report only the latter here.

To distinguish "true" decay dynamics from instances of viral rebound due to, for example, drug resistance or poor treatment adherence, we required that the VL data maintain a consistent decreasing trend toward suppression, such that each measurement was no greater than 500 copies mL^{-1} above the previous one. This buffer region ensured that infants were not excluded from the analysis because of transient increases in VL arising from noise and measurement error. Although the buffer could in principle allow gradual, sustained increases in VL over time, there were no such cases in our study. Finally, to accommodate early increases in VL arising from pharmacological delays in drug action, we began each decreasing sequence at the maximum value of the first 3 measurements. With these criteria, 53 infants were suitable for analysis (see Fig. 1 and Fig. S1, Supplemental Digital Content, http://links.lww.com/QAI/B497). Of these, 49 were initially prescribed a drug regimen of 3 reverse transcriptase inhibitors (RTIs). The remaining 4 were treated with a protease inhibitor and 2 RTIs (details in Supplemental Digital Content, http://links.lww.com/QAI/B497). All infants were switched to a protease inhibitor–based regimen at a median age of 31 days.

Model

We describe HIV decline in an infant on ART using a standard ordinary differential equation model that characterizes the production and spread of virus by infected target cells, such as CD4 T cells (see Supplemental Digital Content, http://links.lww.com/QAI/B497).[16–20] Assuming RTIs completely block viral replication, and that cell-free virus is cleared over a much shorter timescale than the lifespan of infected cells, the time course of VL, V, during treatment can be described by

$$V(t) = A\exp(-\delta t) + B\exp(-\gamma t). \quad (1)$$

Here, t represents the infant age, and δ and γ are the death rates of short-lived and long-lived infected target cells, respectively.[18] We do not explicitly include the dynamics of latently infected cells because we assume their contribution to VL, relative to short-lived and long-lived infected cells,

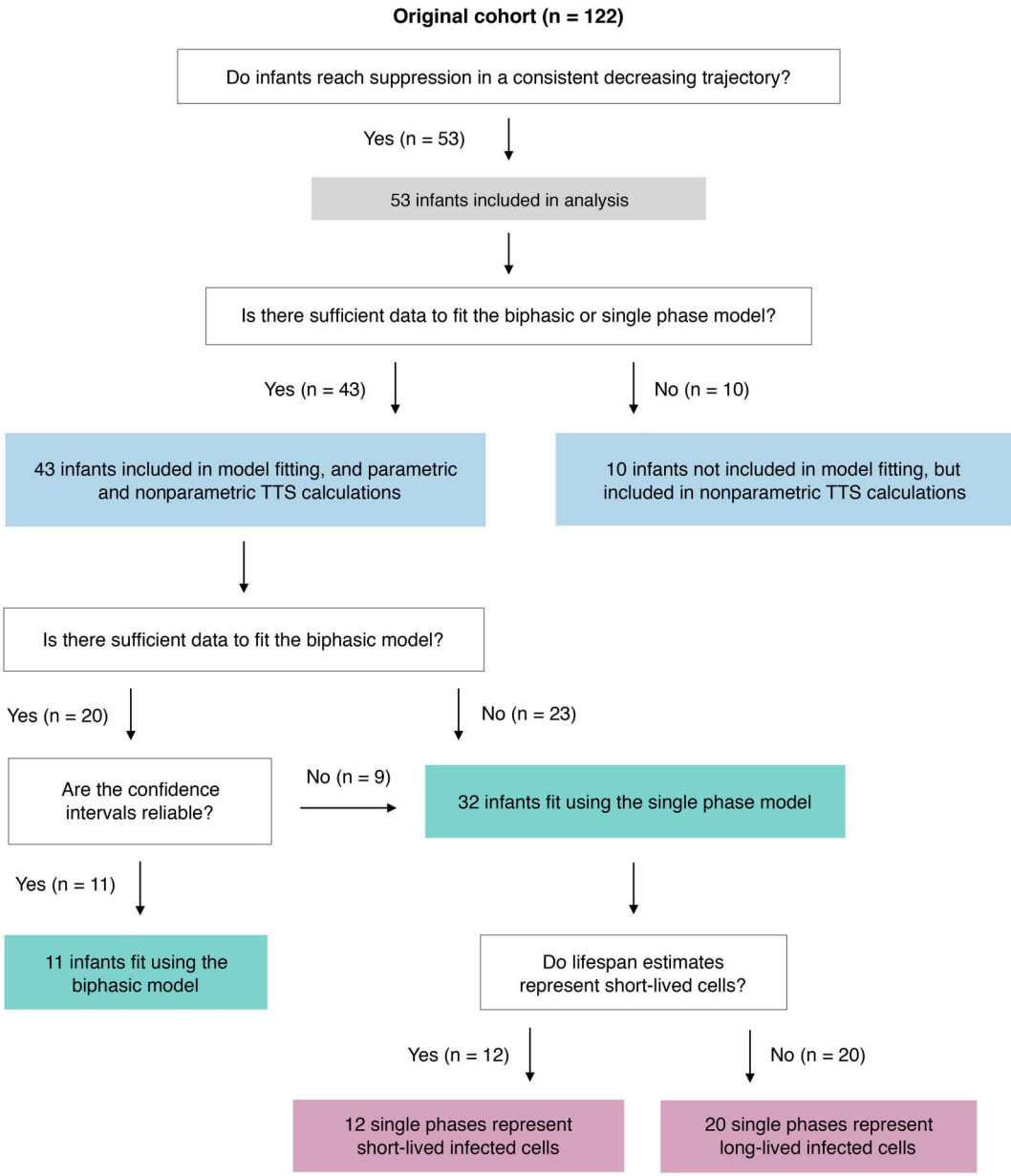

FIGURE 1. Structure of data analysis. Infants from the original study were partitioned into different analysis subsets according to specific criteria. White outlined boxes represent the partitioning criteria and shaded boxes describe the resulting subsets. "Reliable confidence intervals" are confidence intervals on parameter estimates that do not exceed 2 orders of magnitude. TTS stands for time to suppression.

is minimal for the duration of the study.[16] The parameters A and B are composite constants (see Supplemental Digital Content, http://links.lww.com/QAI/B497), where A + B represents the initial VL (ie, V (t = 0)), and A/(A + B) is the proportion of infected cells at ART initiation that are short-lived.

We refer to Equation 1 as the biphasic model, in which VL initially decays rapidly, reflecting the loss of short-lived infected cells (at rate δ), and then enters a second, slower decline phase reflecting the loss of longer-lived infected cells (at rate γ). The transition between these phases occurs when their gradients are equal,[25] giving the following expression for the phase transition time, T_t (see Supplemental Digital Content, http://links.lww.com/QAI/B497),

$$T_t = \frac{\log(A\delta) - \log(B\gamma)}{\delta - \gamma}. \quad (2)$$

For infant data exhibiting only 1 decline phase (eg, because

of sparse or delayed VL measurements), we use a single-phase version of Equation 1,

$$V(t) = \widehat{B}\exp(-\widehat{\gamma}t), \quad (3)$$

and make no assumption regarding whether this reflects the fast or slow phase of virus suppression.

Time to Suppression (TTS)

We estimated the time for each infant to reach virologic suppression ("time to suppression", or TTS) using both parametric and nonparametric methods. For the parametric approach, TTS was calculated as the time for V(t) to reach 20 copies mL^{-1}, where V(t) is given by Equation 1 for the biphasic model and Equation 3 for the single phase model. For the nonparametric approach, we applied linear interpolation between the first measurement below the detection threshold and the preceding measurement. TTS was then defined as the time at which the interpolation line crossed the detection threshold. All TTS estimates are quoted in days since ART initiation.

Model Fitting and Analyses

We obtained parameter estimates with 95% confidence intervals for each infant by fitting either the biphasic or single phase model to the corresponding VL data using a maximum likelihood approach in R.[26,27] Data were $\log_{10}$ transformed before fitting and assessed for normality using the Shapiro–Wilk test. After fitting, model residuals were assessed for autocorrelation, and no statistically significant results were found (see Supplemental Digital Content, http://links.lww.com/QAI/B497). The biphasic model was used only if there were at least 5 measurements above the detection threshold, and the single phase model was used for infants with between 3 and 5 such measurements. Some of the latter showed large differences in VL between the first and second measurements, suggesting an unobserved transition from the fast to the slow decay phase. To prevent such occurrences biasing the estimated single slope of decay, we removed the first measurement if the difference in VL was greater than 10^4 copies mL^{-1}. Finally, infants with fewer than 3 measurements above the detection threshold were excluded from the parametric fitting procedure but were included in the nonparametric TTS calculations. All code for model fitting is available through the ushr package in R.[28]

In addition to the above individual-based approach, we also used nonlinear mixed effects modeling to fit the biphasic equation to data from all 53 infants who met our inclusion criteria, regardless of the number of available measurements.[29] The nonlinear mixed effects approach gave similar results to those obtained when fitting each infant independently (see Supplemental Digital Content, http://links.lww.com/QAI/B497). For clarity, we present results from the individual-based approach, which provides unconstrained estimates of parameters and the correlations between them.

After fitting each model, we used the resulting parameter estimates to calculate the lifespans of short-lived and long-lived infected cells ($1/\delta$ and $1/\gamma$, respectively) and the initial fraction of infected cells that were short-lived ($A/(A + B)$). We also tested for associations between fitted parameters, baseline covariates, and TTS estimates using Spearman correlations for numerical covariates and the Kruskal–Wallis test for categorical covariates. We controlled for multiple comparisons using the Benjamini–Hochberg correction.[30] To aid in clinical interpretation, some numerical covariates were also stratified as categorical variables. For example, CD4 percentages were partitioned into those below or above 35% to represent infants with or without symptoms of HIV-associated immunodeficiency, respectively.[31] For a full list of stratifications see Table S3, Supplemental Digital Content, http://links.lww.com/QAI/B497. We note that CD4 count and percentage measurements were unavailable for 12 of the 53 infants included in our analyses.

RESULTS

Characterizing the Kinetics of Viral Decay on ART

Of the 53 infants included in our analysis, 43 had at least 3 VL measurements above the detection threshold and were modeled using the biphasic or single phase equations (Fig. 1). Although 20 of these infants had sufficient data to fit the biphasic model, 9 subsequently yielded at least 1 parameter with unreliable confidence intervals that spanned over 2 orders of magnitude, likely because of inadequate sampling during one of the decay phases (see Fig. S2, Supplemental Digital Content, http://links.lww.com/QAI/B497). We therefore refit the data from these 9 infants using the single phase model. Biphasic model fits and parameter estimates for the 11 remaining infants are given in Figures 2 and 3A, and Table S1, Supplemental Digital Content, http://links.lww.com/QAI/B497. The median lifespan of short-lived infected cells was 3.2 days (SD = 4.4 days), with an average half-life of 2.2 days (SD = 3.1 days). The corresponding estimates for long-lived infected cells were 31.4 days (SD = 49.8 days) and 21.8 days (SD = 34.5 days), respectively, and the median time from ART initiation to the phase transition was 22 days (SD = 34.4 days). The timing of this transition was unrelated to the timing of changes in ART regimen (Fig. 2, vertical grey lines), indicating that it is not a treatment-specific effect. In addition, the distribution of $A/(A + B)$ was tightly centered around 0.99 (median = 0.99, SD = 0.02). Therefore, almost all infectious virus is produced by short-lived infected cells at ART initiation.

When testing for associations between model parameters and infant covariates, we found A, B, and A + B were highly correlated with $\log_{10}$ baseline VL (correlations = 0.97, 0.82, and 0.98, respectively; all corresponding P-values < 0.05). This is unsurprising as A and B determine the initial VL predicted by the model. Although we did not detect significant associations between the decay rates (δ and γ) and any infant covariates, we did find that δ and γ were positively correlated with each other (correlation = 0.68, $P = 0.025$). In

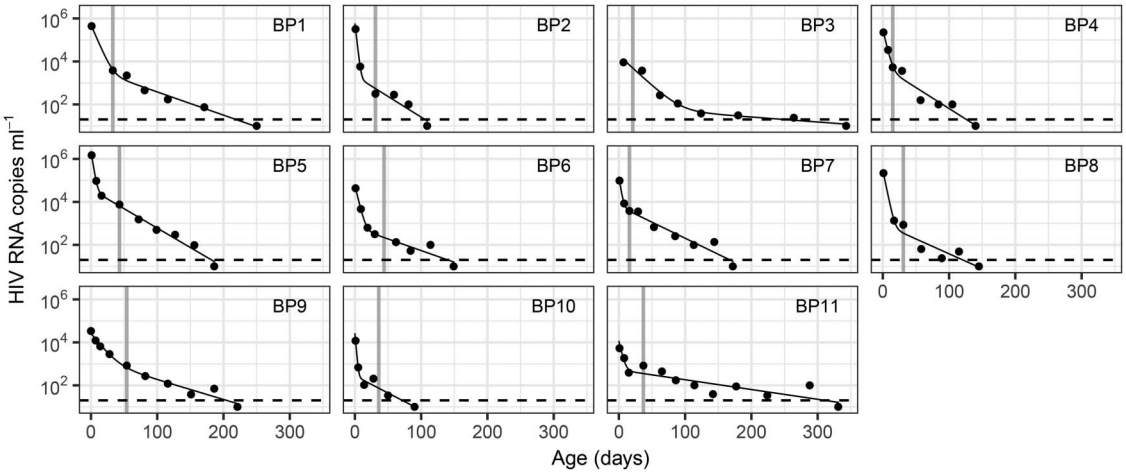

FIGURE 2. Eleven infants fit using the biphasic model. Each panel represents a different infant (ID inset top right; BP stands for "biphasic"). Points represent VL data, black solid lines are the biphasic model fits, and dashed horizontal lines indicate the assay detection threshold. The phase transition occurs when the first decline phase meets the second, and the time at which the drug regimen changed is depicted by the vertical grey line.

other words, infants with a slow first phase are more likely to have a slow second phase.

In total, data from 32 infants were fit using the single phase model (see Figs. 1 and 4, and Table S2, Supplemental Digital Content, http://links.lww.com/QAI/B497). For 14 infants with large differences in VL between the first and second measurements, the first data point was removed before fitting, as discussed above (see also Fig. S3, Supplemental Digital Content, http://links.lww.com/QAI/B497). The single phase decay rate estimates yielded a median infected cell lifespan of 23.7 days (SD = 16.8 days), corresponding to a half-life of 16.4 days (SD = 11.7 days). However, the distribution of estimates spanned those of the short-lived and long-lived lifespans obtained from the biphasic model (Fig. 3B), suggesting some of the observed single phase trajectories represent the first decline phase and some represent the second. To account for this, we first defined a cutoff threshold of 18 days that (i) partitioned the short-lived and long-lived estimates from the biphasic model and (ii) defined a natural break in the distribution of estimates from the single phase model, with 12 below the threshold and 20 above (Figs. 3A, B, dashed vertical line). Subsequently combining partitions from the single and biphasic distributions gave a median lifespan of 7.1 days (SD = 5.4 days, n = 23) for short-lived infected cells and 31.4 days (SD = 32 days, n = 31) for long-lived infected cells (Fig. 3C). The corresponding half-life estimates were 5 days (SD = 3.8 days) and 21.8 days (SD = 22.2 days), respectively. Using alternative partition criteria did not substantially impact these results (see Supplemental Digital Content, http://links.lww.com/QAI/B497).

Finally, we exploited the larger sample size of the combined partition estimates to test for additional associations between clinical covariates and infected cell lifespans. This revealed a negative correlation between the lifespan of short-lived infected cells and $\log_{10}$ baseline VL (correlation = -0.56, $P = 0.03$; see Fig. S4, Supplemental Digital Content, http://links.lww.com/QAI/B497), suggesting infants with higher VL experience more rapid decay during the initial decline phase. We note, however, that the significance of this association was reduced to a trend (correlation = -0.5, $P = 0.09$) when infant SP16, an outlier with the lowest VL and second longest cell lifespan, was removed from the analysis.

TTS

TTS estimates from the parametric and nonparametric methods were in close correspondence (correlation = 0.96, $P < 2 \times 10^{-16}$, n = 43; Fig. 5A). We therefore conducted all TTS analyses using the nonparametric estimates, for which there was a greater sample size (n = 53; Fig. 1). The median TTS was 105 days (SD = 72 days; Fig. 5B), and TTS was marginally inversely associated with baseline CD4 percentage (correlation = -0.36, $P = 0.057$; Fig. 5C). In addition, TTS was positively correlated with $\log_{10}$ baseline VL (correlation = 0.40, $P = 0.01$; Fig. 5D), suggesting higher VL delays virus suppression. We did not detect significant associations between TTS and any of the stratified categorical covariates (see Table S3, Supplemental Digital Content, http://links.lww.com/QAI/B497). Finally, for the 11 infants fit using the biphasic model, TTS was negatively correlated with the decay rate of long-lived infected cells, γ (correlation = -0.81, $P = 0.016$). This result held when the corresponding estimates from the single phase model were also included (Fig. 3C, right panel; correlation = -0.55, $P = 0.015$, n = 31) and is unsurprising given that the decay rate of long-lived infected cells determines the rate of approach to suppression.

DISCUSSION

In this study, we captured HIV decline in perinatally infected infants on ART using a model of biphasic exponential decay. Similar models have been applied in studies of adults and other young infants undergoing treatment.[16,18,21,22,32,33] Despite

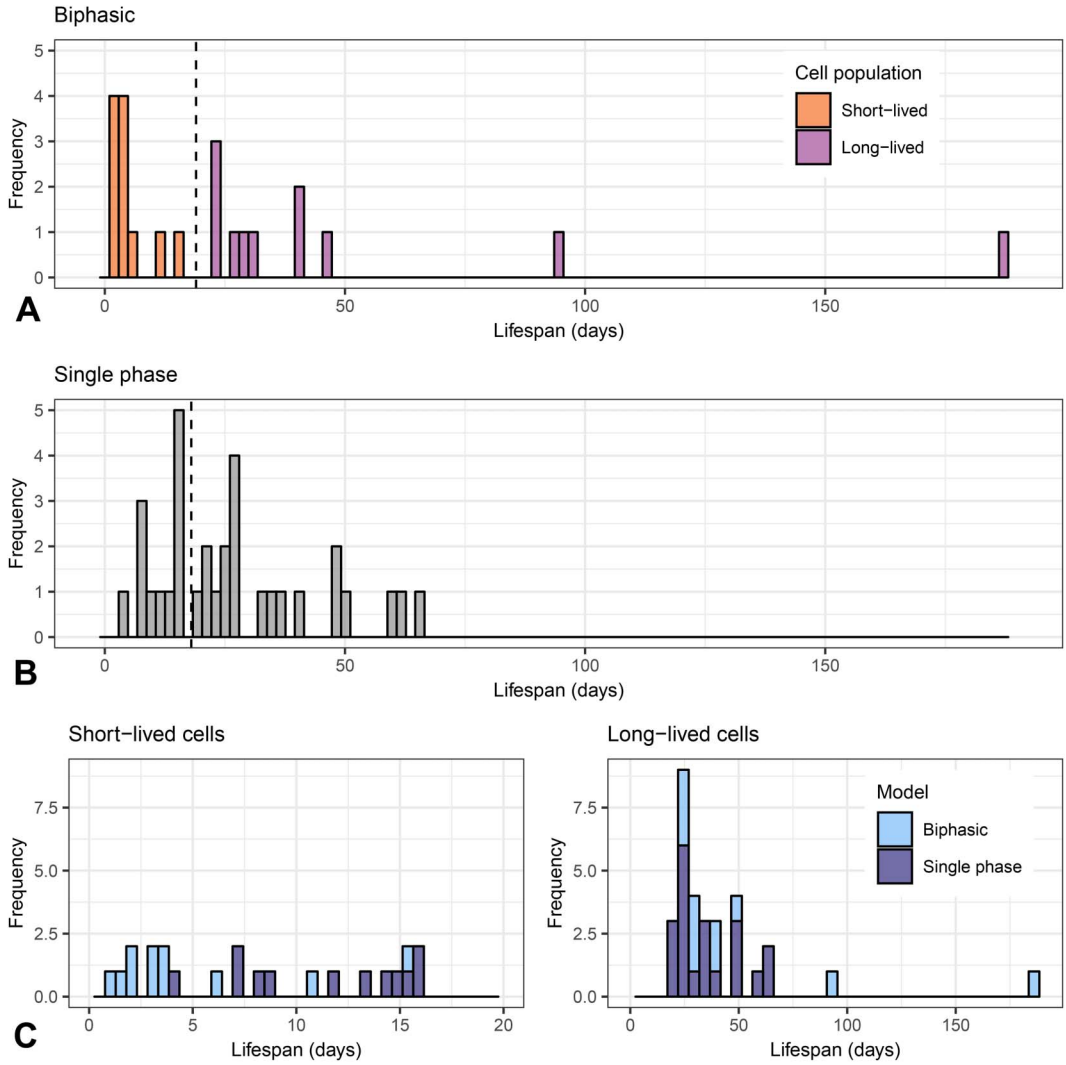

FIGURE 3. Distribution of infected cell lifespans. A, Estimates from the biphasic model (n = 11). The short-lived lifespan was calculated as $1/\delta$, and the long-lived lifespan as $1/\gamma$. The dashed vertical line represents the cutoff threshold separating the short-lived and long-lived distributions. B, Estimates from the single phase model (n = 32) were calculated as $1/\widehat{\gamma}$. The dashed vertical line represents the cutoff threshold defined in (A). C, Combined distributions of the estimated lifespan of short-lived cells (left; n = 23) and long-lived cells (right; n = 31) after partitioning the single phase estimates in (B) according to the cutoff threshold.

substantial variation in findings both within and across these studies, they provide useful context for the results presented here. Firstly, our median estimates of the lifespan of short-lived infected cells (3.2 days for the biphasic model and 7.1 days for the combined biphasic and single phase estimates) are greater than those derived from acute and chronically infected adults (1–1.5 days) and infants under 3 months of age (1.8 days).[16,17,21,22,33] The 95% confidence interval on our combined short-lived estimates also eclipses those of previous work, although there is partial overlap with the subset from the biphasic model (see Fig. S5, Supplemental Digital Content, http://links.lww.com/QAI/B497). A number of biological factors may underlie a longer cell lifespan in neonates, including (1) poorer drug efficacy and/or adherence, (2) a less potent immune response, and (3) different phenotypic characteristics of susceptible target cells.[13,34–36] However, perhaps a more parsimonious explanation is that by only fitting the model to infants with sufficient data, our estimates are biased toward those with longer, and thus more well-documented, first decay phases (see Supplemental Digital Content, http://links.lww.com/QAI/B497).

By contrast, our estimates of the lifespan of long-lived infected cells (31 days for both the biphasic model and the combined estimates) are consistent with those from other age groups (25 days for infants under 3 months and 21–35 days for acute and chronically infected adults).[16,18,22,33] The 95% confidence intervals around our estimates also encompass those of previous work (see Fig. S5, Supplemental Digital Content, http://links.lww.com/QAI/B497). Similarly, our estimates for A/(A + B) (0.99), the timing of the phase transition (22 days), and TTS (105 days) are consistent with those in adults (0.94–0.99, 2–3 weeks, and 125 days, respectively).[16–18,22,33,37] Collectively, these findings suggest

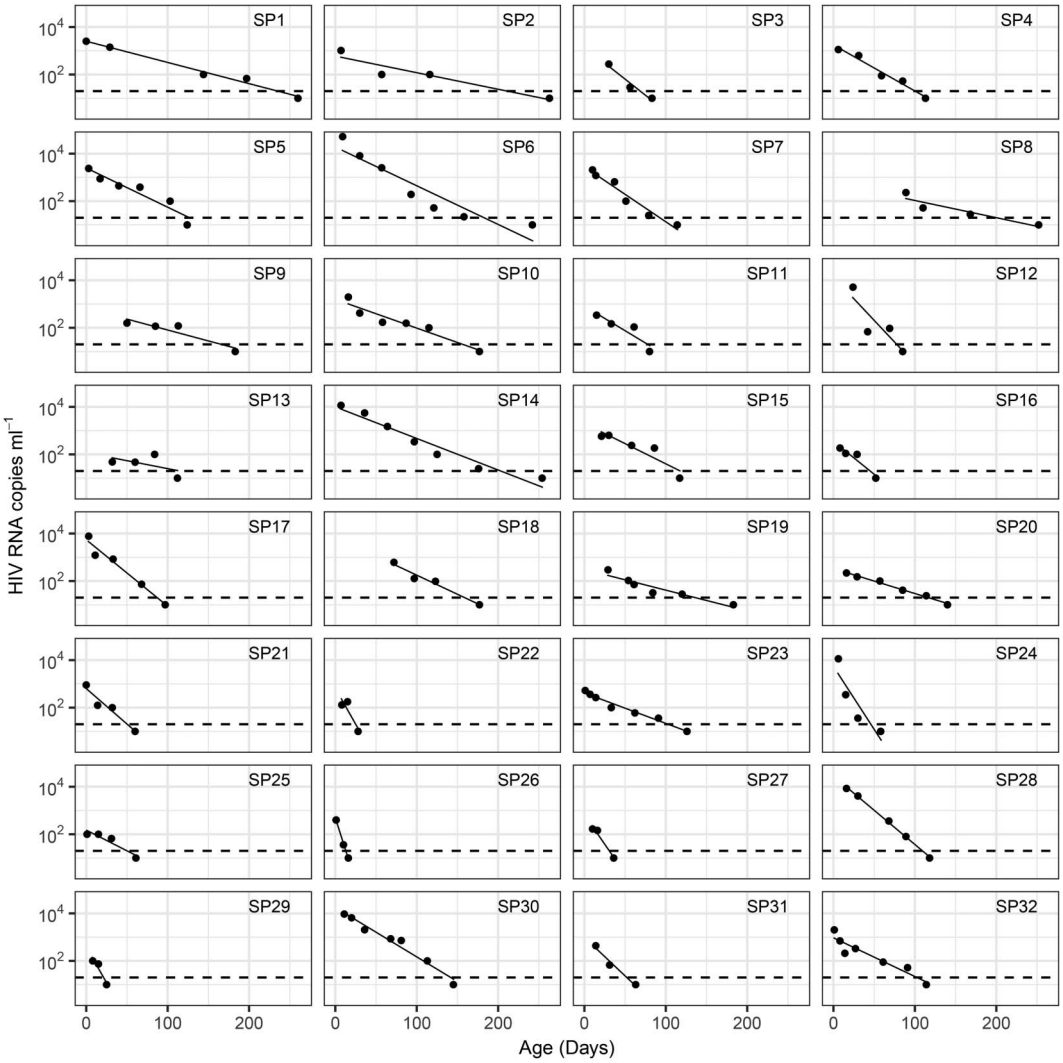

FIGURE 4. Thirty-two infants fit using the single phase model. Each panel represents a different infant (ID inset top right; SP stands for "single phase"). Points represent the VL data, solid lines are the single phase model fits, and dashed horizontal lines indicate the assay detection threshold.

that young infants are largely similar to other age groups in their dynamics of HIV decay during ART.

When testing for statistical associations, we found a trend toward infants with higher baseline CD4 percentage achieving faster suppression. Although not strictly significant ($P = 0.057$), the effect magnitude is substantial and echoes findings from other perinatally infected infants,[12,38] and studies in older children that link higher CD4 percentage to increased probability of viral suppression and reduced risk of mortality.[39,40] Although baseline CD4 counts are also strongly linked to disease progression in chronically infected adults,[40–43] we did not detect any relationship between TTS and CD4 counts. However, this is unsurprising given that CD4 counts in young infants are more variable than CD4 percentages.[31]

In addition to CD4 percentage, we found that baseline VL was moderately associated with both TTS and the lifespan of short-lived infected cells. The correlation between baseline VL and TTS has been observed previously in perinatally infected infants[12,38,44] and is to be expected given that those with higher VLs have "further to fall" before suppressing HIV. By contrast, the correlation between higher VLs and reduced cell lifespans (ie, faster initial decay rates) is less well defined. First, our analysis suggested this association may be partly influenced by one infant with a particularly low VL. Second, although a number of studies in chronically infected adults have connected higher VLs to faster decay rates,[37,45] others in adults and young infants have found no such association.[21,22,46] In addition, we note that baseline VL in chronically infected adults (analogous to the set-point VL) reflects the severity of HIV infection at steady state, whereas the corresponding measurement in infants and acutely infected adults represents a snapshot of infection during a highly dynamic period. Therefore, baseline VL may be an unreliable indicator of initial HIV burden in young infants.

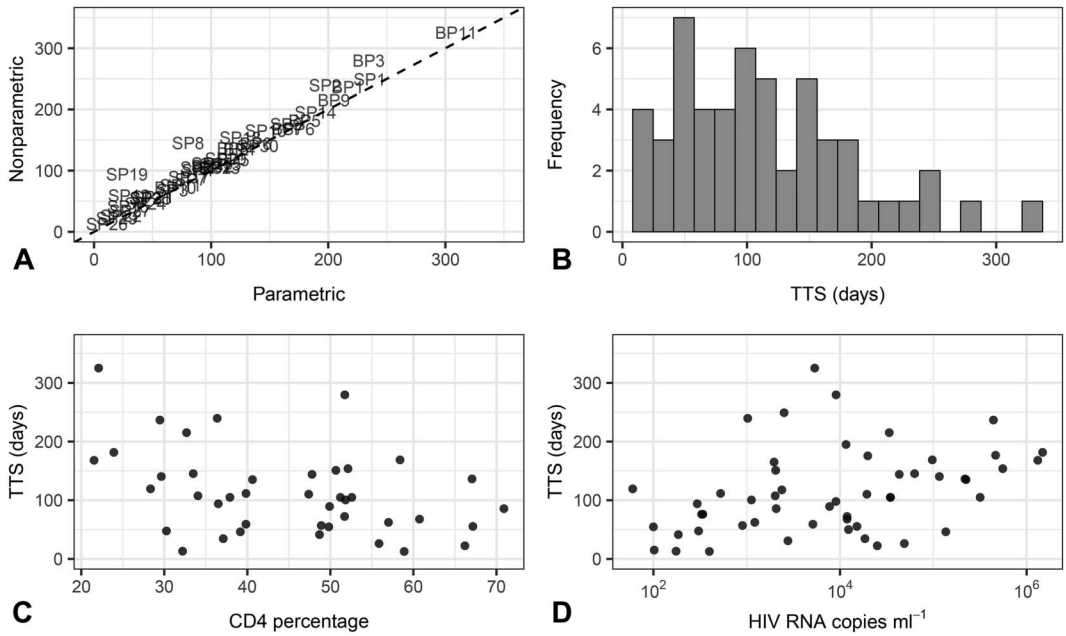

FIGURE 5. TTS is associated with baseline CD4 percentage and VL. A, Comparison of TTS estimation by parametric and nonparametric methods for 43 infants fit using the biphasic or single phase models (correlation = 0.96, $P < 2 \times 10^{-16}$). Estimates are reported in days since ART initiation, and each infant is represented by their corresponding ID (BP stands for "biphasic" and SP for "single phase"). B, Distribution of nonparametric TTS estimates (in days) for all 53 infants who reached viral suppression. C, Association between nonparametric TTS and baseline CD4 percentage (correlation = −0.36, $P = 0.057$). Twelve of the 53 infants were not included due to missing CD4 percentage measurements. D, Association between nonparametric TTS and $\log_{10}$ baseline VL for all 53 infants (correlation = 0.40, $P = 0.01$).

Aside from CD4 percentage and baseline VL, we did not detect strong associations between any other model parameters or infant covariates. In particular, we did not detect an effect of age at ART initiation, which was previously associated with faster decay rates and earlier viral suppression in young infants.[5,12,22,38,47] This inconsistency may be partly due to the highly skewed distribution of age at ART initiation in our study (for 53 infants included in the analysis: median = 2 days, IQR = 1–7 days) compared with previous work (eg, median = 3.8 months, IQR = 2.8–11.3 months[22]; and median = 2.9 months, IQR = 1.4–4.1 months[12,38]). In other words, our lack of infants with later treatment initiation may reduce the discriminatory power of this variable.

Finally, we note a number of caveats to our modeling approach. First, to obtain the biphasic expression (Eqn. 1) we assume that cell-free virus dynamics occur on a much faster timescale than those of infected cells. In adults, this is reasonable as free virus in blood has a half-life of less than 2 hours.[48] However, the extent to which this applies in young infants has not been directly assessed. Although alternative models estimate virus half-life by including an additional exponential decay term (similar to the terms for short-lived and long-lived infected cells),[17,19] fitting this term requires extensive sampling immediately after ART initiation and is thus not feasible for neonates. Second, the model assumes RTIs are completely effective in blocking viral replication, and we do not distinguish between the efficacy of different drug combinations. Whether these factors hold true in neonates is unclear, although challenges to drug efficacy include possible underlying drug resistance, incomplete adherence and suboptimal dosing.[23,49] If some replication continues during ART, the true decline in infected cells will be partially masked by new virion production. As a consequence, the model will underestimate the loss of infected cells and overestimate infected cell lifespans.[32] It is therefore possible that incomplete effectiveness of RTIs during the neonatal period contributes to our increased estimates of short-lived infected cell lifespans compared with those in adults.

In summary, we used an established mathematical model to capture HIV decline in perinatally infected neonates initiating early ART. Using this framework, we estimated key biological parameters and found that very young infants are broadly similar to older age groups in infection kinetics. Our findings contribute to the growing body of research on HIV progression and treatment in neonates and highlight how quantitative approaches can be harnessed to better understand disease dynamics.

ACKNOWLEDGMENTS

Data were collected during the Latency and Early Neonatal Provision of Antiretroviral Drugs Clinical Trial (LEOPARD) study. The LEOPARD study was supported in part by the Eunice Kennedy Shriver National Institute of Child Health and Human Development/National Institute of Allergy and Infectious Disease, National Institutes of Health

(U01HD080441), USAID/PEPfAR, the South African National HIV Programme, and South African Research Chairs Initiative of the Department of Science and Technology and National Research Foundation of South Africa.

The authors thank the infants and families who participated in the study, in addition to the LEOPARD study team: Louise Kuhn, Elaine Abrams, Wei-Yann Tsai, and Stephanie Shiau (Columbia University Medical Center, NY); Caroline Tiemessen, Maria Paximadis, Sharon Shalekoff, Diana Schramm, and Gayle Sherman (National Institute of Communicable Diseases (NICD), Johannesburg, South Africa); Renate Strehlau, Megan Burke, Martie Conradie, Ashraf Coovadia, Ndileka Mbete, Faeezah Patel, and Karl Technau (Empilweni Services and Research Unit (ESRU), Rahima Moosa Mother and Child Hospital, Johannesburg, South Africa); Grace Aldrovandi (University of CA, Los Angeles); Rohan Hazra (Eunice Kennedy Shriver National Institute of Child Health and Human Development); and Devasena Gnanashanmugam (National Institutes of Allergy and Infectious Diseases).

The authors also thank the EPIICAL Consortium study team: Nigel Klein, Diana Gibb, Sarah Watters, Man Chan, Laura McCoy, and Abdel Babiker (University College London, United Kingdom); Anne-Genevieve Marcelin and Vincent Calvez (Université Pierre et Marie Curie, France); Maria Angeles Munoz (Servicio Madrileño de Salud-Hospital General Universitario Gregorio Marañon, Spain); Britta Wahren (Karolinska Institutet, Sweden); Caroline Foster (Imperial College Healthcare NHS Trust, London, United Kingdom); Mark Cotton (Stellenbosch University-Faculty of Medicine and Health Sciences, South Africa); Merlin Robb and Jintanat Ananworanich (The Henry M. Jackson Foundation for the Advancement of Military Medicine, MD); Polly Claiden (HIV i-Base, United Kingdom); Deenan Pillay (University of KwaZulu-Natal Africa Center, South Africa); Deborah Persaud (Johns Hopkins University); Rob J de Boer, Juliane Schröter, and Anet J N Anelone (University of Utrecht, Netherlands); Thanyawee Puthanakit (Thai Red Cross AIDS-Research Centre, Thailand); Adriana Ceci and Viviana Giannuzzi (Consorzio per Valutazioni Biologiche e Farmacologiche, Italy); Katherine Luzuriaga (University of Massachusetts Medical School, Worcester, MA); Nicolas Chomont (Centre de Recherche du Centre Hospitalier de l'Université de Montreal-University of Montreal, Canada); Mark Cameron (Case Western Reserve University, Cleveland, OH); Caterina Cancrini (Università degli Studi di Roma Tor Vergata, Italy); Andrew J Yates, Louise Kuhn, and Sinead E Morris (Columbia University Medical Center, NY); Avy Violari and Kennedy Otwombe (University of the Witwatersrand, Johannesburg [PHRU], South Africa); Ilaria Pepponi and Francesca Rocchi (Children's Hospital "Bambino Gesu", Rome, Italy); Stefano Rinaldi (University of Miami, Miller School of Medicine, FL); Alfredo Tagarro (Hospital 12 de Octubre, Universidad Complutense, Madrid, Spain); Maria Grazia Lain and Paula Vaz (Fundação Ariel Glaser contra o SIDA Pediátrico, Mozambique); and Elisa Lopez and Tacita Nhampossa (Fundação Manhiça, Mozambique).

REFERENCES

1. Global Burden of Disease Collaborative Network. Global, regional, and national age-sex-specific mortality for 282 causes of death in 195 countries and territories, 1980–2017: a systematic analysis for the Global Burden of Disease Study 2017. *Lancet.* 2018;392:1736–1788.
2. Global Burden of Disease Collaborative Network. *Global Burden of Disease Study 2017 (GBD 2017) Results*; 2018. Available at: http://ghdx.healthdata.org/gbd-results-tool. Accessed February 21, 2019.
3. Chiappini E, Galli L, Tovo PA, et al. Virologic, immunologic, and clinical benefits from early combined antiretroviral therapy in infants with perinatal HIV-1 infection. *AIDS.* 2006;20:207–215.
4. Violari A, Cotton MF, Gibb DM, et al. Early antiretroviral therapy and mortality among HIV-infected infants. *N Engl J Med.* 2008;359:2233–2244.
5. Goetghebuer T, Chenadec JL, Haelterman E, et al. Short- and long-term immunological and virological outcome in HIV-infected infants according to the age at antiretroviral treatment initiation. *Clin Infect Dis.* 2012;54:878–881.
6. Cotton MF, Violari A, Otwombe K, et al. Early time-limited antiretroviral therapy versus deferred therapy in South African infants infected with HIV: results from the children with HIV early antiretroviral (CHER) randomised trial. *Lancet.* 2013;382:1555–1563.
7. Luzuriaga K, Tabak B, Garber M, et al. HIV type 1 (HIV-1) proviral reservoirs decay continuously under sustained virologic control in HIV-1–infected children who received early treatment. *J Infect Dis.* 2014;210:1529–1538.
8. Martínez-Bonet M, Puertas MC, Fortuny C, et al. Establishment and replenishment of the viral reservoir in perinatally HIV-1-infected children initiating very early antiretroviral therapy. *Clin Infect Dis.* 2015;61:1169–1178.
9. van Zyl GU, Bedison MA, van Rensburg AJ, et al. Early antiretroviral therapy in South African children reduces HIV-1-infected cells and cell-associated HIV-1 RNA in blood mononuclear cells. *J Infect Dis.* 2015;212:39–43.
10. McManus M, Mick E, Hudson R, et al. Early combination antiretroviral therapy limits exposure to HIV-1 replication and cell-associated HIV-1 DNA levels in infants. *PLoS One.* 2016;11:e0154391.
11. Shiau S, Strehlau R, Technau KG, et al. Early age at start of antiretroviral therapy associated with better virologic control after initial suppression in HIV-infected infants. *AIDS.* 2018;31:355–364.
12. Chan MK, Goodall R, Judd A, et al. Predictors of faster virological suppression in early treated infants with perinatal HIV from Europe and Thailand. *AIDS.* 2019;33:1155–1165.
13. Kuhn L, Shiau S. The pharmacological treatment of acute HIV infections in neonates. *Expert Rev Clin Pharmacol.* 2017;10:1353–1361.
14. Newell MI, Coovadia H, Cortina-Borja M, et al. Mortality of infected and uninfected infants born to HIV-infected mothers in Africa: a pooled analysis. *Lancet.* 2004;364:1236–1243.
15. Ho DD, Neumann AU, Perelson AS, et al. Rapid turnover of plasma virions and CD4 lymphocytes in HIV-1 infection. *Nature.* 1995;373:123–126.
16. Perelson AS, Essunger P, Cao Y, et al. Decay characteristics of HIV-1-infected compartments during combination therapy. *Nature.* 1997;387:188–191.
17. Wu H, Ding AA. Population HIV-1 dynamics in vivo: applicable models and inferential tools for virological data from AIDS clinical trials. *Biometrics.* 1999;55:410–418.
18. Shet A, Nagaraja P, Dixit NM. Viral decay dynamics and mathematical modeling of treatment response: evidence of lower in vivo fitness of HIV-1 subtype C. *J Acquir Immune Defic Syndr.* 2016;73:245–251.
19. Perelson AS, Neumann AU, Markowitz M, et al. HIV-1 dynamics in vivo: virion clearance rate, infected cell life-span, and viral generation time. *Science.* 1996;271:1582–1586.
20. Nowak MA, May RM. *Virus Dynamics: Mathematical Principles of Immunology and Virology*. New York, NY: Oxford University Press; 2000.
21. Markowitz M, Louie M, Hurley A, et al. A novel antiviral intervention results in more accurate assessment of human immunodeficiency virus type 1 replication dynamics and T-cell decay in vivo. *J Virol.* 2003;77:5037–5038.
22. Luzuriaga K, Wu H, McManus M, et al. Dynamics of human immunodeficiency virus type 1 replication in vertically infected infants. *J Virol.* 1999;73:362–367.

23. Kuhn L, Strehlau R, Shiau S, et al. Early antiretroviral treatment of infants to attain HIV remission. *EClinicalMedicine* 2020;18:100241.
24. Wu H, Kuritzkes DR, McClernon DR, et al. Characterization of viral dynamics in human immunodeficiency virus type 1-infected patients treated with combination antiretroviral therapy: relationships to host factors, cellular restoration, and virologic end points. *J Infect Dis.* 1999; 179:799–807.
25. Wu H, Connick E, Kuritzkes DR, et al. Multiple CD4+ cell kinetic patterns and their relationships with baseline factors and virological responses in HIV type 1 patients receiving highly active antiretroviral therapy. *AIDS Res Hum Retroviruses.* 2001;17:1231–1240.
26. R Core Team. *R: A Language and Environment for Statistical Computing*. Vienna, Austria: R Foundation for Statistical Computing; 2019.
27. Hogan T, Gossel G, Yates AJ, et al. Temporal fate mapping reveals age-linked heterogeneity in naive T lymphocytes in mice. *Proc Natl Acad Sci.* 2015;112:E6917–E6926.
28. Morris SE, Dziobek-Garrett L, Yates AJ. Ushr: understanding suppression of HIV in R. *BMC Bioinformatics.* 2020;21:1–8.
29. Comets E, Lavenu A, Lavielle M. Parameter estimation in nonlinear mixed effect models using saemix, an R implementation of the SAEM algorithm. *J Stat Softw.* 2017;80:1–41.
30. Benjamini Y, Hochberg Y. Controlling the false discovery rate: a practical and powerful approach to multiple testing. *J R Stat Soc Ser B Stat Methodol.* 1995;57:289–300.
31. World Health Organization. *WHO Case Definitions of HIV for Surveillance and Revised Clinical Staging and Immunological Classification of HIV-Related Disease in Adults and Children*. Geneva, Switzerland: WHO; 2007.
32. Ding AA, Wu H. Relationships between antiviral treatment effects and biphasic viral decay rates in modeling HIV dynamics. *Math Biosci.* 1999; 160:63–82.
33. Kilby JM, Lee HY, Hazelwood JD, et al. Treatment response in acute/early infection versus advanced AIDS: equivalent first and second phases of HIV RNA decline. *AIDS.* 2008;22:957–962.
34. Burns DN, Mofenson LM. Paediatric HIV-1 infection. *Lancet.* 1999;354: SII1–SII6.
35. Palumbo P, Lindsey JC, Hughes MD, et al. Antiretroviral treatment for children with peripartum nevirapine exposure. *N Engl J Med.* 2010;363: 1510–1520.
36. Violari A, Lindsey JC, Hughes MD, et al. Nevirapine versus ritonavir-boosted lopinavir for HIV-infected children. *N Engl J Med.* 2012;366: 2380–2389.
37. Notermans DW, Goudsmit J, Danner SA, et al. Rate of HIV-1 decline following antiretroviral therapy is related to viral load at baseline and drug regimen. *AIDS.* 1998;12:1483–1490.
38. Schröter J, Anelone AJN, Yates AJ, et al. Time to viral suppression in perinatally HIV-infected infants depends on the viral load and CD4 T-cell percentage at the start of treatment. *J Acquir Immune Defic Syndr.* 2020;83:522–529.
39. van Dijk JH, Sutcliffe CG, Munsanje B, et al. HIV-infected children in rural Zambia achieve good immunologic and virologic outcomes two years after initiating antiretroviral therapy. *PLoS One.* 2011;6:1–8.
40. Jiamsakul A, Kariminia A, Althoff KN, et al. HIV viral load suppression in adults and children receiving antiretroviral therapy—results from the IeDEA collaboration. *J Acquir Immune Defic Syndr.* 2017;76:319–329.
41. Mellors JW, Muñoz A, Giorgi JV, et al. Plasma viral load and CD4+ lymphocytes as prognostic of HIV-1 infection. *Ann Intern Med.* 1997;126:946–954.
42. Egger M, May M, Chêne G, et al. Prognosis of HIV-1-infected patients starting highly active antiretroviral therapy: a collaborative analysis of prospective studies. *Lancet.* 2002;360:119–129.
43. Mujugira A, Celum C, Tappero JW, et al. Younger age predicts failure to achieve viral suppression and virologic rebound among HIV-1-infected persons in serodiscordant partnerships. *AIDS Res Hum Retroviruses.* 2016;32:148–154.
44. Prendergast A, Mphatswe W, Tudor-Williams G, et al. Early virological suppression with three-class antiretroviral therapy in HIV-infected African infants. *AIDS.* 2008;22:1333–1343.
45. Hughes RA, Sterne JAC, Walsh J, et al. Predicting virological decay in patients starting combination antiretroviral therapy. *AIDS.* 2016;30: 1817–1827.
46. Bonhoeffer S, Funk GA, Günthard HF, et al. Glancing behind virus load variation in HIV-1 infection. *Trends Microbiol.* 2003;11:499–504.
47. Veldsman KA, van Rensburg AJ, Isaacs S, et al. HIV-1 DNA decay is faster in children who initiate ART shortly after birth than later. *J Int AIDS Soc.* 2019;22:e25368.
48. Ramratnam B, Bonhoeffer S, Binley J, et al. Rapid production and clearance of HIV-1 and hepatitis C virus assessed by large volume plasma apheresis. *Lancet.* 1999;354:1782–1785.
49. Maswabi K, Ajibola G, Bennett K, et al. Safety and efficacy of starting antiretroviral therapy in the first week of life. *Clin Infect Dis.* 2020; ciaa028:1–6.